

# Enhanced tonic GABA<sub>A</sub> inhibition in typical absence epilepsy

David W Cope<sup>1</sup>, Giuseppe Di Giovanni<sup>1,2</sup>, Sarah J Fyson<sup>1</sup>, Gergely Orbán<sup>1,2</sup>, Adam C Errington<sup>1</sup>, Magor L Lőrincz<sup>1</sup>, Timothy M Gould<sup>1</sup>, David A Carter<sup>1</sup> & Vincenzo Crunelli<sup>1</sup>

The cellular mechanisms underlying typical absence seizures, which characterize various idiopathic generalized epilepsies, are not fully understood, but impaired  $\gamma$ -aminobutyric acid (GABA)-ergic inhibition remains an attractive hypothesis. In contrast, we show here that extrasynaptic GABA<sub>A</sub> receptor-dependent ‘tonic’ inhibition is increased in thalamocortical neurons from diverse genetic and pharmacological models of absence seizures. Increased tonic inhibition is due to compromised GABA uptake by the GABA transporter GAT-1 in the genetic models tested, and GAT-1 is crucial in governing seizure genesis. Extrasynaptic GABA<sub>A</sub> receptors are a requirement for seizures in two of the best characterized models of absence epilepsy, and the selective activation of thalamic extrasynaptic GABA<sub>A</sub> receptors is sufficient to elicit both electrographic and behavioral correlates of seizures in normal rats. These results identify an apparently common cellular pathology in typical absence seizures that may have epileptogenic importance and highlight potential therapeutic targets for the treatment of absence epilepsy.

Typical absence seizures characterize numerous idiopathic generalized epilepsies and appear in the electroencephalogram (EEG) as bilaterally synchronous spike-and-wave discharges (SWDs) accompanied by behavioral arrest<sup>1,2</sup>. Whereas absence seizures are known to arise in thalamo-cortical networks<sup>2–4</sup>, the underlying cellular mechanisms are not fully understood. Impaired GABAergic inhibition remains an attractive hypothesis<sup>5,6</sup>, and GABA<sub>A</sub> receptor (GABA<sub>A</sub>R) subunit mutations have been identified in human cohorts with typical absence seizures, albeit as part of a complex phenotype<sup>7–9</sup>. However, although some of these mutations compromise GABA<sub>A</sub>R function in heterologous expression systems<sup>10</sup>, only modest changes in GABA<sub>A</sub>R inhibition have so far been identified in the thalamo-cortical network of rodents with spontaneous SWDs<sup>11–13</sup>. Furthermore, systemic or intrathalamic administration of agents that promote GABAergic inhibition, including the antiepileptic drugs vigabatrin and tiagabine, initiate or exacerbate seizures in humans and rodents<sup>14–18</sup>. Thus, augmented rather than impaired GABA<sub>A</sub>R inhibition may be a feature of absence seizures.

Activation of GABA<sub>A</sub>Rs generates two types of inhibition: the transient activation of synaptic GABA<sub>A</sub>Rs (sGABA<sub>A</sub>Rs) elicits inhibitory postsynaptic currents (IPSCs), or ‘phasic’ inhibition; and the activation of peri- or extrasynaptic GABA<sub>A</sub>Rs (eGABA<sub>A</sub>Rs) by ambient GABA causes a persistently active, or tonic, current<sup>19,20</sup>. Because in thalamocortical neurons, major players in thalamo-cortical networks during SWDs, >90% of GABA<sub>A</sub>R inhibition is tonic<sup>21–24</sup>, we have examined the prospect of aberrant tonic inhibition in experimental absence seizures. Our data indicate that enhanced tonic GABA<sub>A</sub> inhibition is a common feature of diverse genetic and

pharmacological models of typical absence epilepsy and may be a requirement for the appearance of absence seizures.

## RESULTS

### Enhanced tonic GABA<sub>A</sub> current in genetic models of absence

Genetic absence epilepsy rats from Strasbourg (GAERS) are a well established polygenic model of absence epilepsy that show bilateral spontaneous SWDs and accompanying behavioral arrest from approximately postnatal day 30 (P30)<sup>16</sup>. In thalamocortical neurons, tonic GABA<sub>A</sub> currents are generated by extrasynaptic receptors containing the  $\delta$  subunit<sup>21–23</sup>, and, in rats,  $\delta$  subunit expression is apparent only from approximately P12 (ref. 25). Therefore, we measured tonic GABA<sub>A</sub> current amplitude from thalamocortical neurons in slices of the somatosensory ventrobasal thalamus of GAERS from P14 onward and compared it to non-epileptic control (NEC) rats of the same age. We observed no significant difference in tonic current amplitude at P14–P16 ( $P > 0.05$  for each day) (Fig. 1a,b). At P17, however, there was an approximately twofold increase in tonic current amplitude in GAERS compared to NEC rats ( $P < 0.05$ ) that was sustained in subsequent days (Fig. 1a,b) and was independent of whole-cell capacitance (Supplementary Results and Supplementary Fig. 1a). Comparison of spontaneous IPSC (sIPSC) parameters in GAERS and NEC rats at the same ages revealed no consistent differences (Supplementary Table 1), in agreement with previous data obtained from younger GAERS<sup>12</sup>. Notably, there was a significantly ( $P < 0.05$ ) smaller sIPSC peak amplitude, frequency, charge transfer and total current in GAERS at P18, but these changes were not maintained at later ages (Supplementary Table 1). These results

<sup>1</sup>School of Biosciences, Cardiff University, Cardiff, UK. <sup>2</sup>Present addresses: Department of Physiology and Biochemistry, Faculty of Medicine and Surgery, University of Malta, Msida, Malta (G.D.) and Dipartimento di Medicina Sperimentale, Sezione di Fisiologia Umana “G. Pagano”, Università di Palermo, Palermo, Italy (G.O.). Correspondence should be addressed to D.W.C. (copedw@cf.ac.uk) or V.C. (crunelli@cf.ac.uk).

Received 21 October 2008; accepted 15 October 2009; published online 22 November 2009; doi:10.1038/nm.2058

**Figure 1** Increased tonic GABA<sub>A</sub> inhibition in genetic and pharmacological models of absence seizures. **(a)** Representative current traces from thalamocortical neurons of P14 (top) and P17 (bottom) NEC rats and GAERS, indicating the presence of tonic GABA<sub>A</sub> currents after the focal application of 100 μM gabazine (GBZ, white bars). Dotted lines indicate the continuation of the initial baseline current for each neuron.

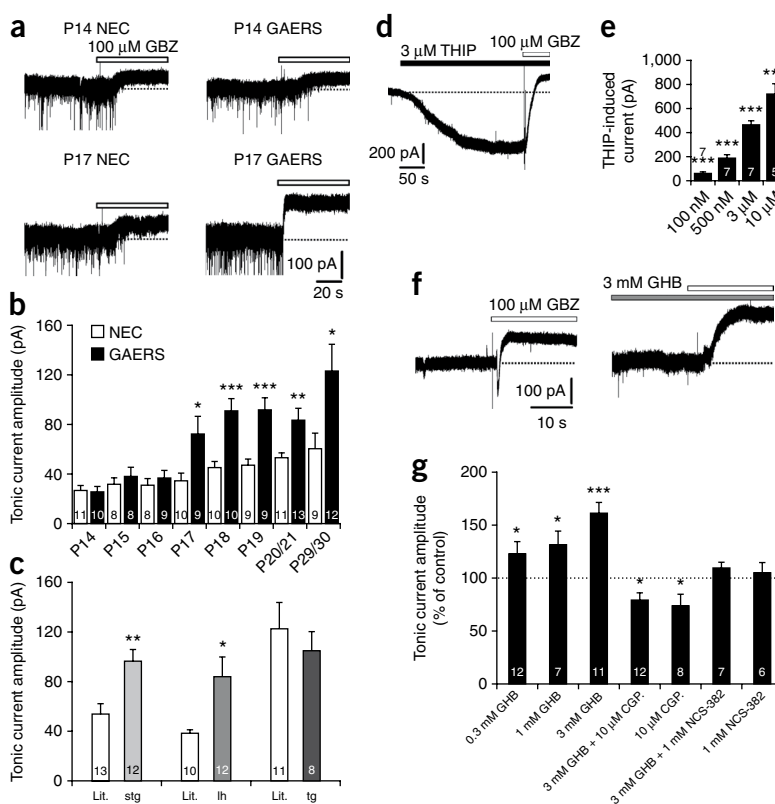
**(b)** Comparison of the tonic current amplitude in NEC rats and GAERS at the indicated ages.

**(c)** Comparison of tonic current amplitude in stargazer (stg, P19–P21), lethargic (lh, P27–P30) and tottering (tg, P26–P28) mice after seizure to respective control littermates of the same age (Lit.).

**(d)** Representative current trace from a normal Wistar rat thalamocortical neuron showing the effect of 3 μM THIP on baseline current in the presence of 0.5 μM tetrodotoxin (TTX). The dotted line indicates the initial baseline current.

**(e)** Comparison of tonic current amplitude in the indicated concentrations of THIP. **(f)** Representative current traces, in the presence of 0.5 μM tetrodotoxin, from two Wistar thalamocortical neurons showing the effect of 3 mM GHB (right) on tonic current amplitude compared to control (left).

**(g)** Comparison of the effects of varying concentrations of GHB on tonic current amplitude and block of GHB-induced increases by the GABA<sub>B</sub>R antagonist CGP55845 (10 μM) and the putative GHB receptor antagonist NCS-382 (1 mM). Values were normalized to the average tonic current amplitude under control conditions. Experiments in **d–g** were performed on P21–P26 Wistar rats. \**P* < 0.05, \*\**P* < 0.01, \*\*\**P* < 0.001. For **b**, **c**, **e** and **g**, the number of recorded neurons is as indicated. Data are presented as means ± s.e.m.



show that thalamocortical neurons of GAERS have a selective enhancement of eGABA<sub>A</sub>R function before seizure onset.

We then tested whether increased tonic GABA<sub>A</sub> current also occurs in the spontaneous mutant mouse strains stargazer, lethargic and tottering, monogenic models of absence epilepsy that have seizures as part of a complex phenotype<sup>26</sup>. In pre-seizure mutant mice, tonic current amplitude measured from thalamocortical neurons in slices of ventrobasal thalamus was not significantly different compared to control littermates (*P* > 0.05) (**Supplementary Fig. 1b**), whereas it was significantly larger in stargazer and lethargic mice after seizure (*P* < 0.01 and *P* < 0.05, respectively) (**Fig. 1c**). However, in tottering mice after seizure, although tonic current amplitude was not significantly different to control littermates, it was of similar magnitude to stargazer and lethargic mice after seizure (**Fig. 1c**). Enhanced tonic current amplitude was still apparent in stargazer and lethargic mice when normalized to whole-cell capacitance (**Supplementary Results and Supplementary Fig. 1d**). Comparison of sIPSC properties revealed no difference between mutant and control littermates either before or after seizure (**Supplementary Table 2**). Thus, as in GAERS, eGABA<sub>A</sub>R function is selectively enhanced in stargazer and lethargic, but not tottering, mice.

### SWD-inducing agents enhance the tonic GABA<sub>A</sub> current

The systemic or intrathalamic administration of  $\gamma$ -hydroxybutyric acid (GHB), a weak GABA<sub>B</sub>R agonist, is an established model of typical absence seizures<sup>27,28</sup>, and the systemic administration of the  $\delta$  subunit-selective agonist 4,5,6,7-tetrahydroisoxazolo[5,4-c]pyridin-3-ol (THIP) has been shown to induce SWDs<sup>29</sup>. Therefore, we tested whether these agents enhance the tonic GABA<sub>A</sub> current in thalamocortical neurons.

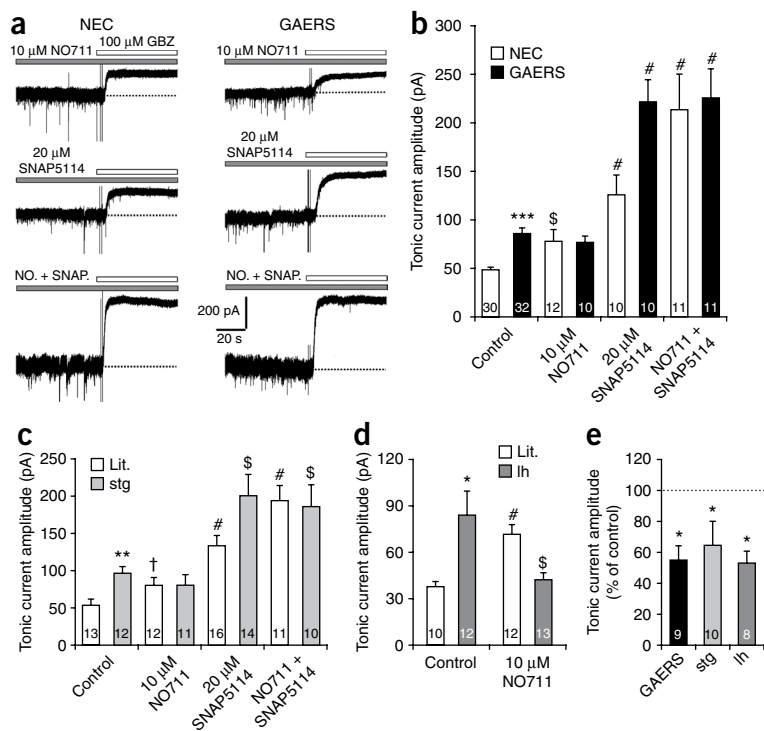
In the presence of tetrodotoxin (0.5 μM), application of 0.1–10 μM THIP increased tonic current amplitude in thalamocortical neurons of the ventrobasal thalamus from normal P21–P26 Wistar rats (all *P* < 0.001) (**Fig. 1d,e**) as described previously for mice<sup>21,23</sup>. Similarly, in the presence of tetrodotoxin, application of 0.3–3 mM GHB, concentrations that induce SWDs *in vivo*<sup>27</sup>, significantly increased tonic current amplitude *in vitro* (all *P* < 0.05) (**Fig. 1f,g**), despite a reduction in IPSC frequency (data not shown)<sup>30</sup>. The action of 3 mM GHB was completely blocked by the GABA<sub>B</sub>R antagonist CGP55845 (10 μM) and the putative GHB antagonist NCS-382 (1 mM) (**Fig. 1g**). Indeed, application of CGP55845 alone significantly reduced tonic current amplitude to 74.0 ± 10.8% of control (*P* < 0.05) (**Fig. 1g**), indicating that facilitation of eGABA<sub>A</sub>Rs by GABA<sub>B</sub>Rs contributes approximately one quarter of the tonic GABA<sub>A</sub> current in normal Wistar rats under control conditions.

These data, together with those from GAERS and stargazer and lethargic mice, show that enhanced eGABA<sub>A</sub>R activity in thalamocortical neurons characterizes diverse genetic and pharmacological models of typical absence seizures.

### GAT-1 malfunction underlies aberrant tonic GABA<sub>A</sub> inhibition

We next examined the mechanism or mechanisms that give rise to enhanced tonic GABA<sub>A</sub> current in GAERS (**Fig. 2**). Elevated GABA levels have been observed in the ventral thalamus of adult GAERS compared to NEC rats<sup>31</sup> and may arise from reduced GABA uptake<sup>32</sup>. Therefore, we tested the contribution of aberrant GABA uptake to enhanced tonic current in P18–P21 GAERS compared to age-matched NEC rats using concentrations of GABA transporter blockers selective for GAT-1 and GAT-3 (ref. 33). In NEC rats, application of the

**Figure 2** Aberrant GABA uptake by GAT-1 underlies enhanced tonic inhibition in GAERS, stargazer and lethargic. **(a)** Representative current traces in P18–P21 NEC rats and GAERS showing the effects of block of GAT-1 alone (after bath application of 10  $\mu$ M NO711, top traces), GAT-3 alone (20  $\mu$ M SNAP5114, middle traces) and GAT-1 and GAT-3 together (NO + SNAP, bottom traces), on tonic current amplitude, revealed by focal application of 100  $\mu$ M GBZ (white bars). **(b)** Comparison of the effects of application of NO711 and SNAP5114 alone, and their application together, on tonic current amplitude in NEC rats and GAERS. **(c)** Comparison of the effect of NO711 and SNAP5114 alone, and their concurrent application, on tonic current amplitude in P19–P21 stargazer mice and control littermates. **(d)** Comparison of the effect of NO711 on tonic current amplitude in P27–P30 lethargic mice and control littermates. **(e)** Comparison of the effect of bath application of 10  $\mu$ M CGP55845 on tonic current amplitude in GAERS and stargazer and lethargic mice. Values were normalized to the average tonic current amplitude in the absence of CGP55845. In **b–d**, \* $P < 0.05$ , \*\* $P < 0.01$  and \*\*\* $P < 0.001$  for mutant versus non-mutant rats or mice under control conditions; † $P < 0.05$ , \$ $P < 0.01$  and # $P < 0.001$  for drug versus non-drug for each strain. In **e**, \* $P < 0.05$  for control versus CGP55845. For **b–e**, the number of recorded neurons is as indicated. Data are presented as means  $\pm$  s.e.m.



GAT-1 blocker NO711 (10  $\mu$ M) significantly increased tonic current compared to control conditions ( $P < 0.01$ ) (Fig. 2a,b), and application of the GAT-3 blocker SNAP5114 (20  $\mu$ M) increased tonic current ( $P < 0.001$ ) to a greater extent than NO711, in agreement with the greater abundance of GAT-3 in the thalamus<sup>34,35</sup>. Concurrent application of NO711 and SNAP5114 in NEC rats increased tonic current ( $P < 0.001$ ) to a greater extent than would be expected by simply summing the effects of NO711 and SNAP5114 alone, suggesting that blocking of GAT-1 causes a compensatory increase in uptake by GAT-3, and vice versa. In GAERS, application of NO711 had no effect on tonic current ( $P > 0.05$ ) (Fig. 2a,b), but application of SNAP5114 caused a large increase ( $P < 0.001$ ). Application of NO711 together with SNAP5114 in GAERS significantly increased tonic current ( $P < 0.001$ ), but the increase was similar to that observed after application of SNAP5114 alone and after application of NO711 and SNAP5114 together in NEC rats (Fig. 2a,b). Compromised GABA uptake by GAT-1 is therefore responsible for enhanced tonic current, as blocking GAT-1 in GAERS had no effect on tonic current amplitude, blocking GAT-1 in NEC rats increased tonic current amplitude to similar values to those seen in GAERS under control conditions, and the compensatory increase in uptake by GAT-1 after blocking GAT-3 is lost in GAERS.

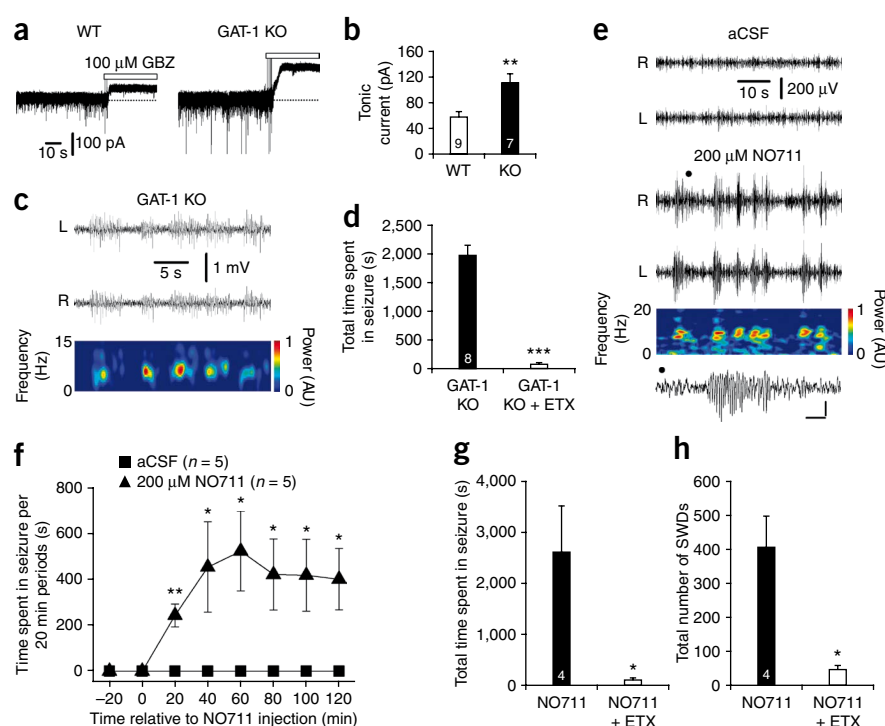
We also tested whether increased vesicular GABA release, over-expression of eGABA<sub>A</sub>Rs, mis-expression of sGABA<sub>A</sub>Rs or aberrant taurine transport contribute to enhanced tonic current in GAERS, but none of these cellular mechanisms were implicated (Supplementary Results and Supplementary Fig. 2). However, because our data in normal Wistar rats showed that activation of GABA<sub>B</sub>Rs contributes to tonic GABA<sub>A</sub> current (Fig. 1g), we tested whether modulation of eGABA<sub>A</sub>Rs by GABA<sub>B</sub>Rs occurs in GAERS. In P18–P21 GAERS, CGP55845 (10  $\mu$ M) significantly reduced tonic current amplitude to  $54.7 \pm 9.5\%$  of control ( $P < 0.05$ ) (Fig. 2e),

indicating that facilitation of eGABA<sub>A</sub> function by GABA<sub>B</sub>R activation contributes almost half of the tonic current in GAERS.

To determine whether compromised GAT-1 activity is restricted to neurons that participate in seizure genesis, we tested the effects of NO711 on tonic GABA<sub>A</sub> current in dentate gyrus granule cells (DGGCs) of GAERS, as the hippocampal formation is not involved in the generation or maintenance of SWDs<sup>16</sup>. Under control conditions, no tonic current was observed in DGGCs of either P18–P21 GAERS or NEC rats (data not shown), and sIPSCs were similar in the two strains (Supplementary Table 3). Application of 10  $\mu$ M NO711, however, induced a tonic current of similar amplitude in both GAERS and NEC rats (Supplementary Fig. 3), indicating that GAT-1 activity is normal in the dentate gyrus of GAERS.

We also tested whether compromised GAT-1 activity underlies enhanced eGABA<sub>A</sub>R function in stargazer and lethargic mice. In stargazer mice, similar to GAERS, there was no effect of GAT-1 block by NO711 on tonic current amplitude, and block of GAT-3 alone by SNAP5114 caused a similar increase to that achieved by application of NO711 and SNAP5114 together ( $P < 0.01$  and  $0.001$ , respectively) (Fig. 2c). In stargazer littermates, NO711 increased tonic current ( $P < 0.05$ ) to the same level as in stargazer mice under control conditions (Fig. 2c). In contrast, in lethargic mice, NO711 significantly decreased tonic current amplitude compared to control conditions ( $P < 0.01$ ), and in lethargic littermates NO711 increased tonic current ( $P < 0.001$ ) to similar values to those seen in lethargic mice under control conditions (Fig. 2d). Thus, in stargazer mice, as in GAERS, increased eGABA<sub>A</sub>R activity is caused by a failure of GABA uptake by GAT-1. However, in lethargic mice, GAT-1 seems to be a source of ambient GABA, implying that GABA transport by GAT-1 is reversed<sup>36</sup>. To test whether GABA<sub>B</sub>R activation contributes to enhanced tonic inhibition in stargazer and lethargic mice, we measured tonic current amplitude in the presence of CGP55845 (10  $\mu$ M). Similarly to the results in GAERS, application of CGP55845 reduced

**Figure 3** Role of thalamic GAT-1 in the generation of SWDs. (a) Representative current traces from P68–P74 WT and GAT-1–knockout (GAT-1 KO) mice indicating the presence of tonic currents after the focal application of 100  $\mu$ M GBZ (white bars). (b) Comparison of tonic current amplitude in WT and GAT-1–knockout (KO) mice. Numbers of recorded neurons are as indicated. (c) Simultaneous, bilateral (L, left hemisphere; R, right hemisphere) EEG traces from a GAT-1–knockout mouse showing spontaneous SWDs under control conditions. At the bottom is a spectrogram corresponding to the R trace. AU, arbitrary units. (d) Comparison of the effect of ethosuximide (ETX) (200 mg per kg body weight i.p.) on the total time (over 1 h) spent in seizure. Number of recorded mice is as indicated. (e) Simultaneous, bilateral EEG traces from a normal Wistar rat after intrathalamic administration of artificial cerebrospinal fluid (aCSF, top traces) and then 200  $\mu$ M NO711 (bottom traces). Second from bottom is a spectrogram for the lowest trace L. At the bottom is an enlargement of the single SWD indicated ( $\bullet$ ). Calibration bars for the enlarged SWD; vertical 200  $\mu$ V, horizontal 1 s. (f) Graph showing the effects of intrathalamic administration of NO711 on the time (20-min periods) spent in seizure, compared to aCSF administration. (g,h) Comparison of the effects of systemic ETX (100 mg per kg body weight i.p.) administration on total time (over 2 h) spent in seizure (g), and total number of SWDs (h), during intrathalamic NO711 administration. \* $P < 0.05$ , \*\* $P < 0.01$  and \*\*\* $P < 0.001$ . Data are presented as means  $\pm$  s.e.m.



tonic current amplitude to  $64.4 \pm 15.7\%$  in stargazer mice and  $52.7 \pm 7.9\%$  in lethargic mice ( $P < 0.05$  for both) (Fig. 2e).

In summary, these data show that increased tonic GABA<sub>A</sub> current in thalamocortical neurons of GAERS and stargazer and lethargic mice is caused by loss of GABA uptake by GAT-1. However, GAT-1 function in DGGCs is unaltered, and GAT-1 expression levels are normal in thalamus and cortex of GAERS (Supplementary Results and Supplementary Fig. 4). We suggest that the resultant increase in ambient GABA in the thalamus leads to enhanced tonic current through direct activation of eGABA<sub>A</sub>Rs and a GABA<sub>B</sub>R-dependent facilitation of eGABA<sub>A</sub>R function.

### Thalamic GAT-1 controls absence seizures

In light of the fact that compromised GAT-1 activity causes enhanced tonic inhibition in thalamocortical neurons of GAERS and stargazer and lethargic mice, we predicted that GAT-1–knockout mice should show both enhanced tonic inhibition and spontaneous SWDs. Tonic current is indeed increased in cerebellar and cortical neurons of GAT-1–knockout mice<sup>37,38</sup>, but thalamocortical neurons have not been tested. Similarly, GAT-1–knockout mice have increased susceptibility to pentylenetetrazole-induced seizures<sup>37</sup>, but the presence of spontaneous SWDs has not been determined. In thalamocortical neurons of P68–P74 GAT-1–knockout mice, tonic current amplitude was significantly larger compared to age-matched wild-type (WT) littermates ( $P < 0.01$ ) (Fig. 3a,b), and normalized tonic current amplitude was also larger ( $P < 0.01$ ) (data not shown). Furthermore, sIPSC properties were also significantly different ( $P < 0.05$ ) (Supplementary Table 3). Freely moving GAT-1–knockout mice showed spontaneous absence seizures, with SWDs having a mean frequency of  $5.2 \pm 0.1$  Hz (range 4.7–5.7 Hz,  $n = 10$  SWDs in each of eight mice) (Fig. 3c) that were blocked by systemic administration of the antiabsence drug ethosuximide (200 mg per kg body weight intraperitoneally (i.p.),  $P < 0.001$ ) (Fig. 3d).

Notably, ethosuximide (750  $\mu$ M) and another antiabsence drug, sodium valproate (500  $\mu$ M), had no effect on tonic current amplitude (Supplementary Fig. 5). Thus, as predicted, GAT-1–knockout mice have both enhanced tonic inhibition in thalamocortical neurons and spontaneous SWDs.

We further tested the role of thalamic GAT-1 in the generation of SWDs by intrathalamic reverse microdialysis of the selective GAT-1 inhibitor NO711 (200  $\mu$ M, effective concentration  $\leq 20$   $\mu$ M, see Online Methods for details) in normal Wistar rats. Application of NO711 induced both behavioral and electrographic correlates of seizures in all rats tested (Fig. 3e,f and Supplementary Movie 1), and SWDs had a mean frequency of  $8.7 \pm 1.3$  Hz (range 5.0–15.3 Hz,  $n = 10$  SWDs from each of five rats). Systemic application of ethosuximide (100 mg per kg body weight i.p.) significantly reduced both the time spent in seizure and the number of SWDs after NO711 administration in all rats tested (Fig. 3g,h) ( $P < 0.05$ ). Thus, intrathalamic NO711 administration is sufficient for the appearance of absence seizures, and these two sets of experiments show that thalamic GAT-1 is crucial in controlling the generation of SWDs.

### eGABA<sub>A</sub>Rs are a requirement for seizure generation

To assess the importance of enhanced eGABA<sub>A</sub>R function to seizure generation in two well established models of absence epilepsy, GHB treatment and GAERS, we performed two sets of experiments. First, we determined whether mice without thalamic eGABA<sub>A</sub>Rs were resistant to the pharmacological induction of absence seizures. GABA<sub>A</sub>  $\delta$  subunit knockout ( $\delta$ -knockout) mice had reduced tonic inhibition in thalamocortical neurons ( $P < 0.01$ ) (Fig. 4a–c)<sup>39</sup>, whereas sIPSCs were largely unaffected (Supplementary Table 3). In WT littermates, systemic administration of the GHB pro-drug  $\gamma$ -butyrolactone (50 mg per kg body weight i.p.)<sup>40</sup> readily induced absence seizures (Fig. 4d,e) that were largely abolished after administration of ethosuximide (200 mg per kg body weight i.p.,



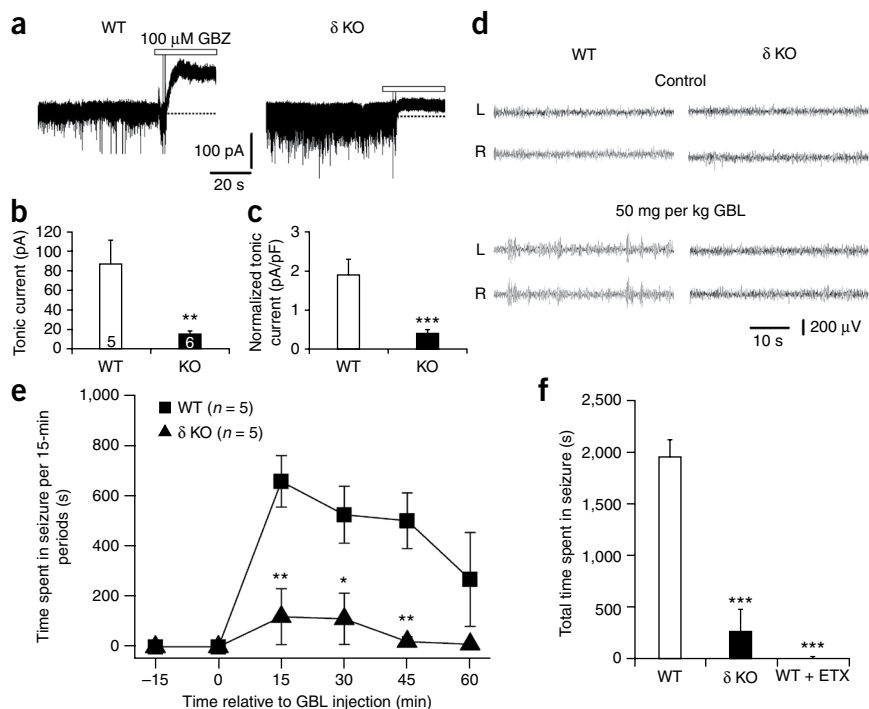


**Figure 4**  $\delta$  subunit–knockout mice show reduced tonic inhibition and reduced sensitivity to  $\gamma$ -butyrolactone (GBL)–induced SWDs. **(a)** Representative current traces from P23–P30 WT (left) and  $\delta$  subunit–knockout ( $\delta$  KO, right) mice revealing tonic currents after the focal application of 100  $\mu$ M GBZ (white bars). **(b)** Comparison of tonic current amplitude in WT and  $\delta$ –knockout (KO) mice. Numbers of recorded neurons are as indicated. **(c)** Comparison of normalized tonic current amplitude for the same neurons as in **b**. **(d)** Simultaneous, bilateral EEG traces from WT and  $\delta$ –knockout mice under control conditions (top) and after injection of GBL (50 mg per kg body weight i.p., bottom). **(e)** Graph showing the effects of GBL on the time (15-min periods) spent in seizure for WT compared to  $\delta$ –knockout mice. **(f)** Comparison of the total time spent in GBL-induced seizure (over 1 h) between WT and  $\delta$ –knockout mice, and the effect of ETX (200 mg per kg body weight i.p.) on seizures in WT mice. The number of recorded mice in **f** is the same as in **e**. \* $P < 0.05$ , \*\* $P < 0.01$  and \*\*\* $P < 0.001$ . Data are presented as means  $\pm$  s.e.m.

$P < 0.001$ ) (Fig. 4f). However,  $\gamma$ -butyrolactone administration only rarely induced SWDs in  $\delta$ –knockout mice (Fig. 4d–f).

In the second set of experiments, we intrathalamically injected  $\delta$  subunit–specific antisense oligodeoxynucleotides in GAERS to knock down  $\delta$  subunit expression and therefore decrease the number of eGABA<sub>A</sub>R $\alpha$ 41. In rats treated with antisense oligodeoxynucleotides (1 or 2 nmol per site), the time spent in seizure and the number of SWDs were significantly reduced ( $P < 0.05$ ) 1–2 d after injection (Fig. 5a,b) compared to control. By comparison, injection of a missense oligodeoxynucleotide (1–2 nmol per site) had no effect on spontaneous seizures (Fig. 5a,b). Notably, injection of the missense oligodeoxynucleotide (2 nmol per site) also had no effect on tonic inhibition in P28–P32 GAERS, compared to age-matched, untreated rats, whereas the antisense oligodeoxynucleotide (2 nmol per site)

significantly reduced tonic current amplitude ( $P < 0.05$ ) (Fig. 5c). Also, neither missense or antisense oligodeoxynucleotides had any effect on sIPSCs (Supplementary Table 3). Oligodeoxynucleotide spread was restricted to the thalamus after *post hoc* visualization of a unilaterally injected biotinylated antisense oligodeoxynucleotide (Fig. 5d). The results from these two sets of experiments demonstrate that enhanced eGABA<sub>A</sub>R function in the thalamus is crucial for the appearance of absence seizures in two of the best characterized models of absence epilepsy.

#### Enhanced eGABA<sub>A</sub>R function is sufficient for absence seizures

To directly test whether enhanced eGABA<sub>A</sub>R function in thalamocortical neurons is sufficient for absence seizures, we used intrathalamic administration of the eGABA<sub>A</sub>R agonist THIP (30–100  $\mu$ M, effective

**Figure 5** Spontaneous absence seizures in GAERS are reduced by intrathalamic injection of  $\delta$  subunit–specific antisense oligodeoxynucleotides (ODNs). **(a)** Graph showing the effect of intrathalamic injection in GAERS of 1 and 2 nmol per site  $\delta$  subunit–specific antisense ODNs and a 1–2 nmol per site non-specific missense ODN on the time spent in seizure. Values were normalized to the time spent in seizure before ODN injection. **(b)** Comparison of the total number of SWDs after antisense (1 nmol per site or 2 nmol per site) and missense (Mis.) ODN administration. Values were normalized to the number of seizures before ODN injection. **(c)** Effect of 2 nmol per site missense and 2 nmol per site antisense administration on tonic current amplitude. Values were normalized to the average tonic current amplitude in age-matched, untreated GAERS. **(d)** Brain section showing that the spread of 2 nmol biotinylated antisense ODN is restricted to the ventrobasal thalamus 24 h after unilateral injection into the right hemisphere. Arrows indicate the termination of the cannulae in both hemispheres. In **a**, \* $P < 0.05$  and \*\* $P < 0.05$  for 1 and 2 nmol antisense ODN, respectively; \*\* $P < 0.01$ . In **b** and **c**, \* $P < 0.05$  and \*\* $P < 0.01$ . The number of rats in **b** is as in **a**. The number of recorded neurons in **c** is as indicated. Data are presented as mean  $\pm$  s.e.m.

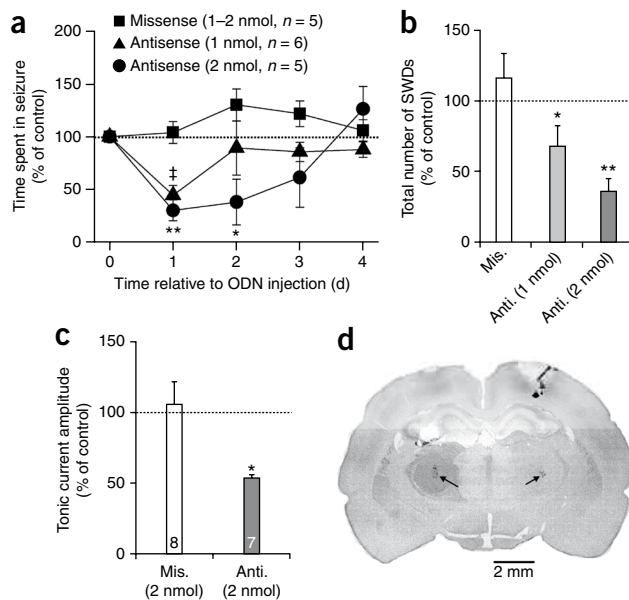


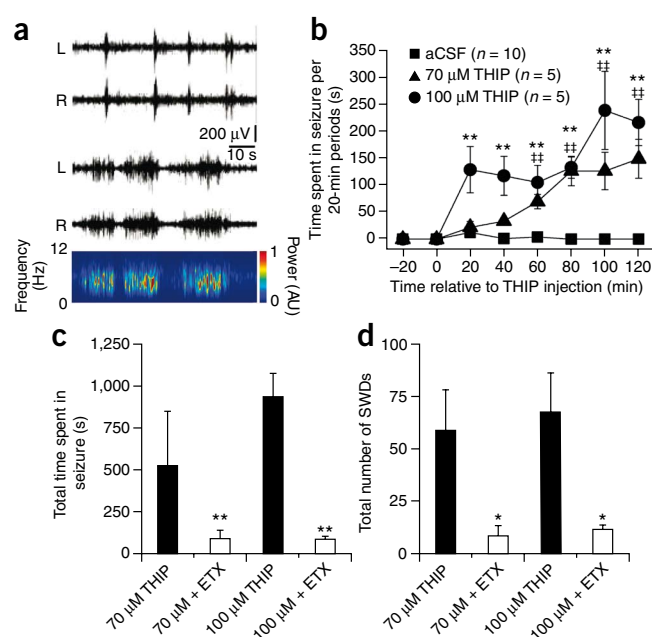
**Figure 6** Selective activation of thalamic eGABA<sub>A</sub>Rs initiates absence seizures in normal Wistar rats. **(a)** Simultaneous, bilateral EEG traces showing representative examples of SWDs in the first (top traces) and second (bottom traces) hour after administration of 100  $\mu$ M THIP in the ventrobasal thalamus. At the bottom is a spectrogram corresponding to the lower R trace. **(b)** Graph showing the effects of intrathalamic administration of 70 and 100  $\mu$ M THIP on the time (20-min periods) spent in seizure, compared to aCSF injection. **(c,d)** Comparison of the effects of systemic ETX (100 mg per kg body weight i.p.) administration on total time (over 2 h) spent in seizure **(c)** and total number of SWDs **(d)** during intrathalamic THIP administration. In **b**, \*\* $P < 0.01$  and †† $P < 0.01$ , for 100 and 70  $\mu$ M THIP versus aCSF, respectively. In **c** and **d**, \* $P < 0.05$  and \*\* $P < 0.01$ . The number of rats in **c** and **d** are the same as indicated in **b**.

concentration  $\leq 3$ –10  $\mu$ M, see Online Methods for details) by reverse microdialysis in normal Wistar rats to determine whether selectively increasing tonic inhibition initiates absence seizures in rats that do not normally have them. THIP induced SWDs in only one out of six rats at low concentrations (30  $\mu$ M, data not shown) but robustly induced the electrographic and behavioral correlates of absence seizures at concentrations of 70 and 100  $\mu$ M (**Fig. 6a,b** and **Supplementary Movie 2**). THIP-induced SWDs had a frequency of  $6.1 \pm 0.9$  Hz (range 5.2–7.5 Hz,  $n = 10$  SWDs in each of four rats), increased in duration during the recording period (**Fig. 6a**), and were blocked by ethosuximide administration (100 mg per kg body weight i.p.,  $P < 0.05$ ) (**Fig. 6c,d**). Because THIP at the concentrations used is selective for  $\delta$  subunit-containing eGABA<sub>A</sub>Rs<sup>42</sup>, our data show that enhanced eGABA<sub>A</sub>R function in thalamocortical neurons is sufficient for the appearance of absence seizures.

## DISCUSSION

Here we have shown that enhanced eGABA<sub>A</sub>R function is a common pathophysiological mechanism in all the diverse genetic and pharmacological models of absence epilepsy tested, except tottering mice (**Supplementary Discussion**). However, in agreement with previous studies, we rarely observed changes in phasic inhibition (**Supplementary Discussion**). Our data also indicate that enhanced tonic inhibition is sufficient for seizure genesis and is a requirement for the appearance of seizures in some models. Previous studies have implicated eGABA<sub>A</sub>Rs and GAT-1 in the generation of convulsive seizures (**Supplementary Discussion**), but our data directly demonstrate a role for both in absence seizures. Moreover, GAT-1-knockout mice and intrathalamic NO711 may represent new models of absence epilepsy. Compromised GAT-1 activity underlies increased tonic inhibition in GAERS and stargazer and lethargic mice, but how the genetic variants in these models lead to GAT-1 malfunction is unknown. GAT-1 is a target for intracellular modulation, at least in neurons<sup>43–46</sup>, but in the thalamus GABA uptake is governed exclusively by astrocytes<sup>34</sup>. Thus, thalamic cellular pathology in absence seizures may be astrocyte specific.

The potential contribution of eGABA<sub>A</sub>Rs to absence seizure generation is considered in the **Supplementary Discussion**. Unexpectedly, in GAERS, stargazer, lethargic and GHB models, a previously unknown GABA<sub>B</sub>R-dependent facilitation of eGABA<sub>A</sub>R function seems to contribute to tonic GABA<sub>A</sub> inhibition. Although the mechanism underlying this facilitation is unknown, our findings help to explain the sensitivity of seizures to GABA<sub>B</sub>R modulation, a defining criterion for models of absence epilepsy, but do not detract from classical pre- and post-synaptic GABA<sub>B</sub>R contributions to seizure genesis (**Supplementary Discussion**).



In conclusion, our data show that enhanced eGABA<sub>A</sub>R function occurs in diverse models of absence seizures and seems to be key in seizure genesis. Furthermore, thalamic GAT-1 crucially controls the appearance of absence seizures. We, therefore, suggest that thalamic eGABA<sub>A</sub>Rs and GABA transporters may be potential targets for the generation of novel therapies against absence seizures.

## METHODS

Methods and any associated references are available in the online version of the paper at <http://www.nature.com/naturemedicine/>.

Note: Supplementary information is available on the Nature Medicine website.

## ACKNOWLEDGMENTS

We thank P. Blanning for his help in genotyping mice, D. Bellelli who kindly provided the genotyping protocol for the  $\delta$  subunit-knockout mice and K. Thomas for initial discussions on the antisense oligodeoxynucleotide experiments. H. Parri, S. Hughes and N. Leresche commented on a previous version of the manuscript. D.W.C. is a research Fellow of Epilepsy Research UK (grant P0802), and G.O. was supported by a Fellowship of the Italian Ministry for University and Scientific Research. This work was also supported by the Wellcome Trust (grant 71436) and the European Union (grant HEALTH F2-2007-202167).

## AUTHOR CONTRIBUTIONS

D.W.C., G.D., S.J.F., A.C.E. and V.C. designed the research; D.W.C., G.D., S.J.F., G.O., A.C.E., M.L.L., T.M.G. and D.A.C. performed the research; D.W.C., G.D., S.J.F., G.O., A.C.E. and D.A.C. analyzed the data; and D.W.C. and V.C. wrote the paper.

Published online at <http://www.nature.com/naturemedicine/>.

Reprints and permissions information is available online at <http://ngp.nature.com/reprintsandpermissions/>.

- Commission on Classification and Terminology of the International League Against Epilepsy. Proposal for revised classification of epilepsies and epileptic syndromes. *Epilepsia* **30**, 389–399 (1989).
- Crunelli, V. & Leresche, N. Childhood absence epilepsy: genes, channels, neurons and networks. *Nat. Rev. Neurosci.* **3**, 371–382 (2002).
- McCormick, D.A. & Contreras, D. On the cellular and network bases of epileptic seizures. *Annu. Rev. Physiol.* **63**, 815–846 (2001).
- Blumenfeld, H. Cellular and network mechanisms of spike-wave seizures. *Epilepsia* **46** Suppl 9, 21–33 (2005).
- von Krosigk, M., Bal, T. & McCormick, D.A. Cellular mechanisms of a synchronized oscillation in the thalamus. *Science* **261**, 361–364 (1993).

6. Huntsman, M.M., Porcello, D.M., Homanics, G.E., DeLorey, T.M. & Huguenard, J.R. Reciprocal inhibitory connections and network synchrony in the mammalian thalamus. *Science* **283**, 541–543 (1999).
7. Wallace, R.H. *et al.* Mutant GABA<sub>A</sub> receptor  $\gamma$ 2-subunit in childhood absence epilepsy and febrile seizures. *Nat. Genet.* **28**, 49–52 (2001).
8. Kananura, C. *et al.* A splice-site mutation in *GABRG2* associated with childhood absence epilepsy and febrile convulsions. *Arch. Neurol.* **59**, 1137–1141 (2002).
9. Maljevic, S. *et al.* A mutation in the GABA<sub>A</sub> receptor  $\alpha$ <sub>1</sub>-subunit is associated with absence epilepsy. *Ann. Neurol.* **59**, 983–987 (2006).
10. Macdonald, R.L., Gallagher, M.J., Feng, H.-J. & Kang, J. GABA<sub>A</sub> receptor epilepsy mutations. *Biochem. Pharmacol.* **68**, 1497–1506 (2004).
11. Caddick, S.J. *et al.* Excitatory but not inhibitory synaptic transmission is reduced in lethargic (*Cacnb4<sup>lh</sup>*) and tottering (*Cacna1a<sup>tg</sup>*) mouse thalami. *J. Neurophysiol.* **81**, 2066–2074 (1999).
12. Bessaïh, T. *et al.* Nucleus-specific abnormalities of GABAergic synaptic transmission in a genetic model of absence seizures. *J. Neurophysiol.* **96**, 3074–3081 (2006).
13. Tan, H.O. *et al.* Reduced cortical inhibition in a mouse model of familial childhood absence epilepsy. *Proc. Natl. Acad. Sci. USA* **104**, 17536–17541 (2007).
14. Hosford, D.A., Wang, Y. & Cao, Z. Differential effects mediated by GABA<sub>A</sub> receptors in thalamic nuclei in *lh/lh* model of absence seizures. *Epilepsy Res.* **27**, 55–65 (1997).
15. Hosford, D.A. & Wang, Y. Utility of the lethargic (*lh/lh*) mouse model of absence seizures in predicting the effects of lamotrigine, vigabatrin, tiagabine, gabapentin and topiramate against human absence seizures. *Epilepsia* **38**, 408–414 (1997).
16. Danober, L., Deransart, C., Depaulis, A., Vergnes, M. & Marescaux, C. Pathophysiological mechanisms of genetic absence epilepsy in the rat. *Prog. Neurobiol.* **55**, 27–57 (1998).
17. Perucca, E., Gram, L., Avanzini, G. & Dulac, O. Antiepileptic drugs as a cause of worsening seizures. *Epilepsia* **39**, 5–17 (1998).
18. Ettinger, A.B. *et al.* Two cases of nonconvulsive status epilepticus in association with tiagabine therapy. *Epilepsia* **40**, 1159–1162 (1999).
19. Farrant, M. & Nusser, Z. Variations on an inhibitory theme: phasic and tonic activation of GABA<sub>A</sub> receptors. *Nat. Rev. Neurosci.* **6**, 215–229 (2005).
20. Glykys, J. & Mody, I. Activation of GABA<sub>A</sub> receptors: views from outside the synaptic cleft. *Neuron* **56**, 763–770 (2007).
21. Belelli, D., Peden, D.R., Rosahl, T.W., Wafford, K.A. & Lambert, J.J. Extrasynaptic GABA<sub>A</sub> receptors of thalamocortical neurons: a molecular target for hypnotics. *J. Neurosci.* **25**, 11513–11520 (2005).
22. Cope, D.W., Hughes, S.W. & Crunelli, V. GABA<sub>A</sub> receptor-mediated tonic inhibition in thalamic neurons. *J. Neurosci.* **25**, 11553–11563 (2005).
23. Jia, F. *et al.* An extrasynaptic GABA<sub>A</sub> receptor mediates tonic inhibition in thalamic VB neurons. *J. Neurophysiol.* **94**, 4491–4501 (2005).
24. Bright, D.P., Aller, M.I. & Brickley, S.G. Synaptic release generates a tonic GABA<sub>A</sub> receptor-mediated conductance that modulates burst precision in thalamic relay neurons. *J. Neurosci.* **27**, 2560–2569 (2007).
25. Laurie, D.J., Wisden, W. & Seeburg, P.H. The distribution of thirteen GABA<sub>A</sub> receptor subunit mRNAs in the rat brain. III. Embryonic and postnatal development. *J. Neurosci.* **12**, 4151–4172 (1992).
26. Fletcher, C.F. & Frankel, W.N. Ataxic mouse mutants and molecular mechanisms of absence epilepsy. *Hum. Mol. Genet.* **8**, 1907–1912 (1999).
27. Snead, O.C., III. The  $\gamma$ -hydroxybutyrate model of absence seizures: correlation of regional brain levels of  $\gamma$ -hydroxybutyric acid and  $\gamma$ -butyrolactone with spike wave discharges. *Neuropharmacology* **30**, 161–167 (1991).
28. Banerjee, P.K., Hirsch, E. & Snead, O.C., III.  $\gamma$ -hydroxybutyric acid induced spike and wave discharges in rats: relation to high-affinity [<sup>3</sup>H] $\gamma$ -hydroxybutyric acid binding sites in the thalamus and cortex. *Neuroscience* **56**, 11–21 (1993).
29. Fariello, R.G. & Golden, G.T. The THIP-induced model of bilateral synchronous spike and wave in rodents. *Neuropharmacology* **26**, 161–165 (1987).
30. Le Feuvre, Y., Fricker, D. & Leresche, N. GABA<sub>A</sub> receptor-mediated IPSCs in rat thalamic sensory nuclei: patterns of discharge and tonic modulation by GABA<sub>B</sub> autoreceptors. *J. Physiol. (Lond.)* **502**, 91–104 (1997).
31. Richards, D.A., Lemos, T., Whitton, P.S. & Bowery, N.G. Extracellular GABA in the ventrolateral thalamus of rats exhibiting spontaneous absence epilepsy: a microdialysis study. *J. Neurochem.* **65**, 1674–1680 (1995).
32. Sutch, R.J., Davies, C.C. & Bowery, N.G. GABA release and uptake measured in crude synaptosomes from Genetic Absence Epilepsy Rats from Strasbourg (GAERS). *Neurochem. Int.* **34**, 415–425 (1999).
33. Borden, L.A. GABA transporter heterogeneity: pharmacology and cellular localization. *Neurochem. Int.* **29**, 335–356 (1996).
34. De Biasi, S., Vitellaro-Zuccarello, L. & Brecha, N.C. Immunoreactivity for the GABA transporter-1 and GABA transporter-3 is restricted to astrocytes in the rat thalamus. A light and electron-microscopic immunolocalization. *Neuroscience* **83**, 815–828 (1998).
35. Pow, D.V. *et al.* Differential expression of the GABA transporters GAT-1 and GAT-3 in brains of rats, cats, monkeys and humans. *Cell Tissue Res.* **320**, 379–392 (2005).
36. Wu, Y., Wang, W., Díez-Sampedro, A. & Richerson, G.B. Nonvesicular inhibitory neurotransmission via reversal of the GABA transporter GAT-1. *Neuron* **56**, 851–865 (2007).
37. Chiu, C.-S. *et al.* GABA transporter deficiency causes tremor, ataxia, nervousness and increased GABA-induced tonic conductance in cerebellum. *J. Neurosci.* **25**, 3234–3245 (2005).
38. Bragina, L. *et al.* GAT-1 regulates both tonic and phasic GABA<sub>A</sub> receptor-mediated inhibition in the cerebral cortex. *J. Neurochem.* **105**, 1781–1793 (2008).
39. Herd, M.B. *et al.* Inhibition of thalamic excitability by 4,5,6,7-tetrahydroisoxazolo [4,5-c]pyridine-3-ol: a selective role for  $\delta$ -GABA<sub>A</sub> receptors. *Eur. J. Neurosci.* **29**, 1177–1187 (2009).
40. Aizawa, M., Ito, Y. & Fukuda, H. Pharmacological profiles of generalized absence seizures in lethargic, stargazer and  $\gamma$ -hydroxybutyrate-treated model mice. *Neurosci. Res.* **29**, 17–25 (1997).
41. Maguire, J.L., Stell, B.M., Rafizadeh, M. & Mody, I. Ovarian cycle-linked changes in GABA<sub>A</sub> receptors mediating tonic inhibition alter seizures susceptibility and anxiety. *Nat. Neurosci.* **8**, 797–804 (2005).
42. Stórustovu, S.I. & Ebert, B. Pharmacological characterization of agonists at  $\delta$ -containing GABA<sub>A</sub> receptors: functional selectivity for extrasynaptic receptors is dependent on the absence of  $\gamma$ 2. *J. Pharmacol. Exp. Ther.* **316**, 1351–1359 (2006).
43. Quick, M.W., Corey, J.L., Davidson, N. & Lester, H.A. Second messengers, trafficking-related proteins and amino acid residues that contribute to the functional regulation of the rat brain GABA transporter GAT1. *J. Neurosci.* **17**, 2967–2979 (1997).
44. Beckman, M.L., Bernstein, E.M. & Quick, M.W. Multiple G protein-coupled receptors initiate protein kinase C redistribution of GABA transporters in hippocampal neurons. *J. Neurosci.* **19**, RC9 (1999).
45. Wang, D., Deken, S.L., Whitworth, T.L. & Quick, M.W. Syntaxin 1A inhibits GABA flux, efflux and exchange mediated by the rat brain GABA transporter GAT1. *Mol. Pharmacol.* **64**, 905–913 (2003).
46. Hu, J. & Quick, M.W. Substrate-mediated regulation of  $\gamma$ -aminobutyric acid transporter 1 in rat brain. *Neuropharmacology* **54**, 309–318 (2008).

## ONLINE METHODS

**Electrophysiological recordings.** We prepared horizontal slices containing the ventrobasal thalamus and dentate gyrus in accordance with the United Kingdom Animals (Scientific Procedures) Act 1986 and associated procedures, as described previously<sup>22</sup>. We made whole-cell patch clamp recordings from visualized ventrobasal thalamocortical neurons and DGGCs held at  $33 \pm 1$  °C, and pipettes were attached to the head stage of either a Multiclamp 700B preamplifier, controlled by Multiclamp Commander software, or an Axopatch 200A preamplifier (Molecular Devices). We measured whole-cell capacitance in response to small (5-mV) voltage pulses. Experimental data were digitized at 20 kHz (Digidata 1322, Molecular Devices), acquired using pClamp 9.0 software (Molecular Devices) and stored on a personal computer. We performed experiments on only a single neuron within a slice, after which we discarded the slice. We bath-applied drugs in the recording medium, except for focal applications of GBZ.

We analyzed data using LabView-based software (National Instruments). Tonic currents were observed as an outward shift in baseline current after application of 100  $\mu$ M GBZ, and we measured tonic and phasic currents as previously described<sup>22</sup>.

**Electroencephalogram recordings in behaving rats and mice.** We performed all surgical procedures in accordance with the UK Animals (Scientific Procedures) Act 1986 and associated procedures. We anesthetized male and female rats and mice of the relevant strains with a mixture of isoflurane and N<sub>2</sub>O, and implanted rats with six screw electrodes placed bilaterally over the frontal cortex, parietal cortex and cerebellum, and mice with four screws bilaterally over the parietal cortex and cerebellum. For injection of antisense and missense oligodeoxynucleotides and reverse microdialysis experiments, we implanted two guide cannulae over the ventrobasal thalamus of rats (anterior-posterior -3.1, lateral 3.0, ventral 4.0; ref. 47) and permanently fixed them to the skull with methylacrylic cement. We checked the position of cannulae *post hoc* (for example, Fig. 5d), and we did not include data from rats with incorrectly positioned cannulae for further analysis. Antisense and missense oligodeoxynucleotides were injected 1 week after recovery from implantation, and we determined the spread of injected oligodeoxynucleotides with a unilaterally injected biotinylated antisense oligodeoxynucleotide visualized by the avidin-biotin-horseradish peroxidase complex procedure (Supplementary Methods). Labeling in the injected hemisphere occurred not only in the ventrobasal thalamus but also in the nucleus reticularis thalami, caudate putamen, central amygdala and some regions of neocortex. However, binding in the caudate putamen, amygdala and neocortex was mirrored in the non-injected hemisphere and is therefore non-specific (Fig. 5d).

For tonic current measurements after oligodeoxynucleotide injection, we killed injected rats 22–26 h after injection and prepared slices as described above. We performed reverse microdialysis experiments after the bilateral insertion of microdialysis probes (CMA/12, 2-mm length and 500- $\mu$ m outer diameter; Carnegie Medicin), connected to a two-channel liquid swivel (Carnegie Medicin), to a depth 2 mm below the end of the cannulae.

We made EEG recordings using a Neurolog (Digitimer Ltd) or Plexon (model REC/64) amplifier, and analyzed data using pClamp 9.0 (Molecular Devices) or Plexon software, respectively. We recorded spontaneous or  $\gamma$ -butyrolactone-induced seizures in mice for a period of 1 h. Control recordings were made before the injection of oligodeoxynucleotides, and experiments started 1 d after injection. For reverse microdialysis experiments, we made EEG recordings first without probes (30 min), second with probes infusing aCSF (20 min, see Supplementary Methods for composition) and third with probes infusing the relevant drug dissolved in aCSF (120 min). Although high concentrations of each drug were used, reverse microdialysis reduces the effective concentration of administered drug to  $\leq 10\%$  (ref. 48), therefore the final concentrations were selective for their desired targets. During the recording session, we video-monitored rats and mice to record the behavioral components of absence seizures. We quantified data as the time spent in seizure during 15-min periods for mice and 20-min periods for rats, and we also calculated the total number of SWDs in some instances. The effect of ethosuximide on spontaneous and drug-induced seizures was tested by i.p. injection at doses of 100–200 mg per kg body weight in a volume of 1 ml kg<sup>-1</sup>.

**Statistical analyses.** For comparison of tonic current amplitude and IPSC properties between mutant and control rats and mice and between neurons recorded under control conditions and in the presence of drugs, we used Student's unpaired *t* test with significance set at  $P < 0.05$ . For EEG recordings, we assessed drug effects by repeated-measures ANOVA with *post hoc* Tukey's honestly significant test when we found significant differences ( $P < 0.05$ ). We compared the effects of ethosuximide on seizures with Student's paired *t* test ( $P < 0.05$ ). All data are presented as means  $\pm$  s.e.m.

**Additional methods.** Detailed methodology is described in the Supplementary Methods.

47. Paxinos, G. & Watson, C. *The Rat Brain in Stereotaxic Coordinates* 2nd edn. (Academic Press, San Diego, 1986).
48. Juhász, G., Kékesi, K., Emri, Z., Soltesz, I. & Crunelli, V. Sleep-promoting action of excitatory amino acid antagonists: a different role for thalamic NMDA and non-NMDA receptors. *Neurosci. Lett.* **114**, 333–338 (1990).

